



Playing Leap-Frog with Pox 186: A Kinematic Case Study of a Local Analog to High-z Star-Forming Galaxies

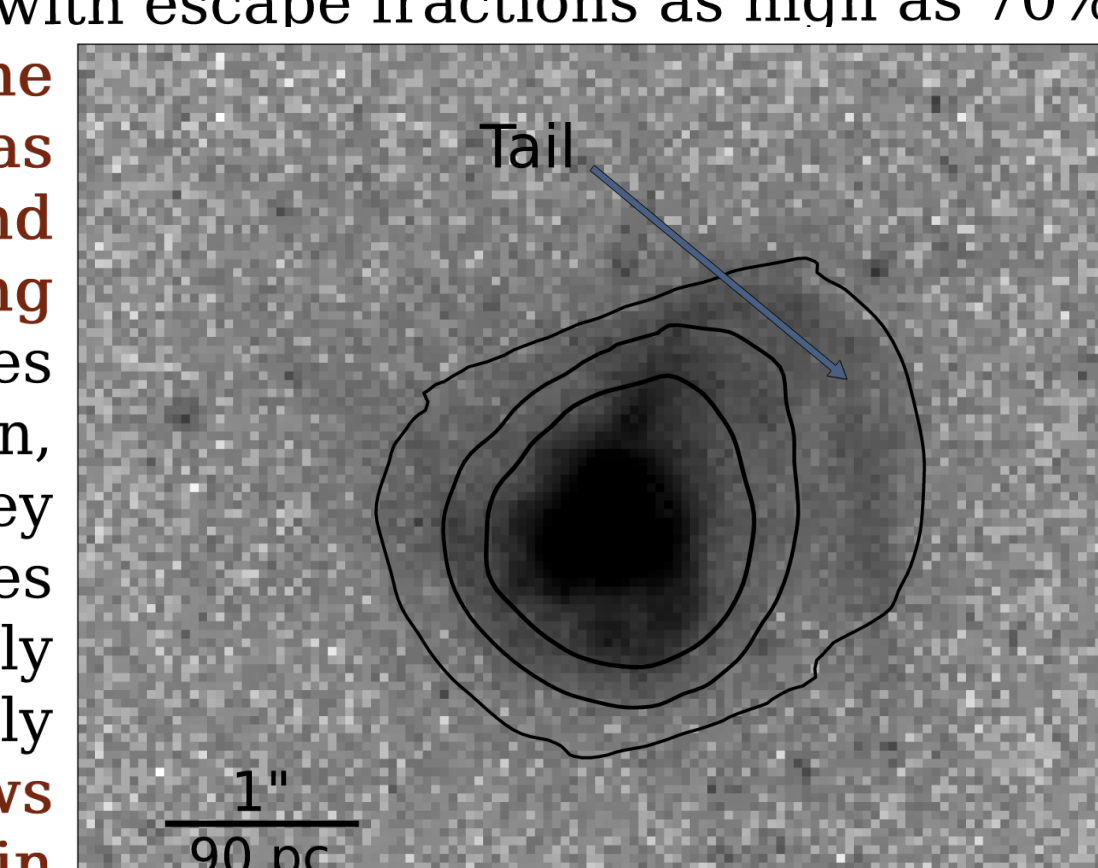
Nathan Eggen¹, Claudia Scarlata¹, Evan Skillman¹, Anne Jaskot²

¹Minnesota Institute for Astrophysics, University of Minnesota-Twin Cities, ²Department of Astronomy, Williams College

① Motivation

Low mass star-forming galaxies are thought to be the primary sources of ionizing photons during the epoch of reionization [1]. A galaxy's capacity to contribute to reionization depends on the total ionizing flux being produced and the fraction that escapes its interstellar medium (f_{esc}), reaching the intergalactic medium (IGM). For reionization to complete by $z \sim 6$, all galaxies must have had an average escape fraction between 10–20% [2]. An increasingly opaque IGM, however, make direct observations of these galaxies escaping ionizing flux difficult. Therefore a set of observables that indicate high escape fractions but are also accessible at $z > 6$ is needed to further constrain the escaping ionizing flux from galaxies responsible for reionization.

Galaxies with high escape fractions have been found among low redshift analogs, the Green Peas. Selected for their high $[\text{OIII}]/[\text{OII}]$ (O_{32}) ratio, Green Peas are compact, highly star-forming galaxies with characteristics similar to those responsible for reionization. Some Green Peas have been found with escape fractions as high as 70% and a strong anti-correlation between the separation of Lyman alpha peaks and f_{esc} has been observed, implying gas kinematics and structure play an important role in determining f_{esc} [3]. Lyman alpha's resonance, however, makes its lineshape difficult to interpret. In addition, Green Peas are limited as useful analogs. They are many times more massive than the galaxies responsible for reionization while simultaneously being too compact and far away to be structurally studied in detail. Looking locally ($z \sim 0$) allows for the detailed mapping of gas kinematics in galaxies with properties analogous to Green Peas, and masses similar to galaxies responsible for reionization. Here we examine one such galaxy, Pox 186.



HST F555W band image with Gemini [OIII] S/N contours of 24, 25, and 26.

② Pox 186 as an Analog

Pox 186 has similar characteristics to Green Peas and 3 pieces of evidence that point to being density bounded, where there is not enough material in the nebula to absorb all ionizing radiation. If entirely density bounded, f_{esc} could reach close to 100%.

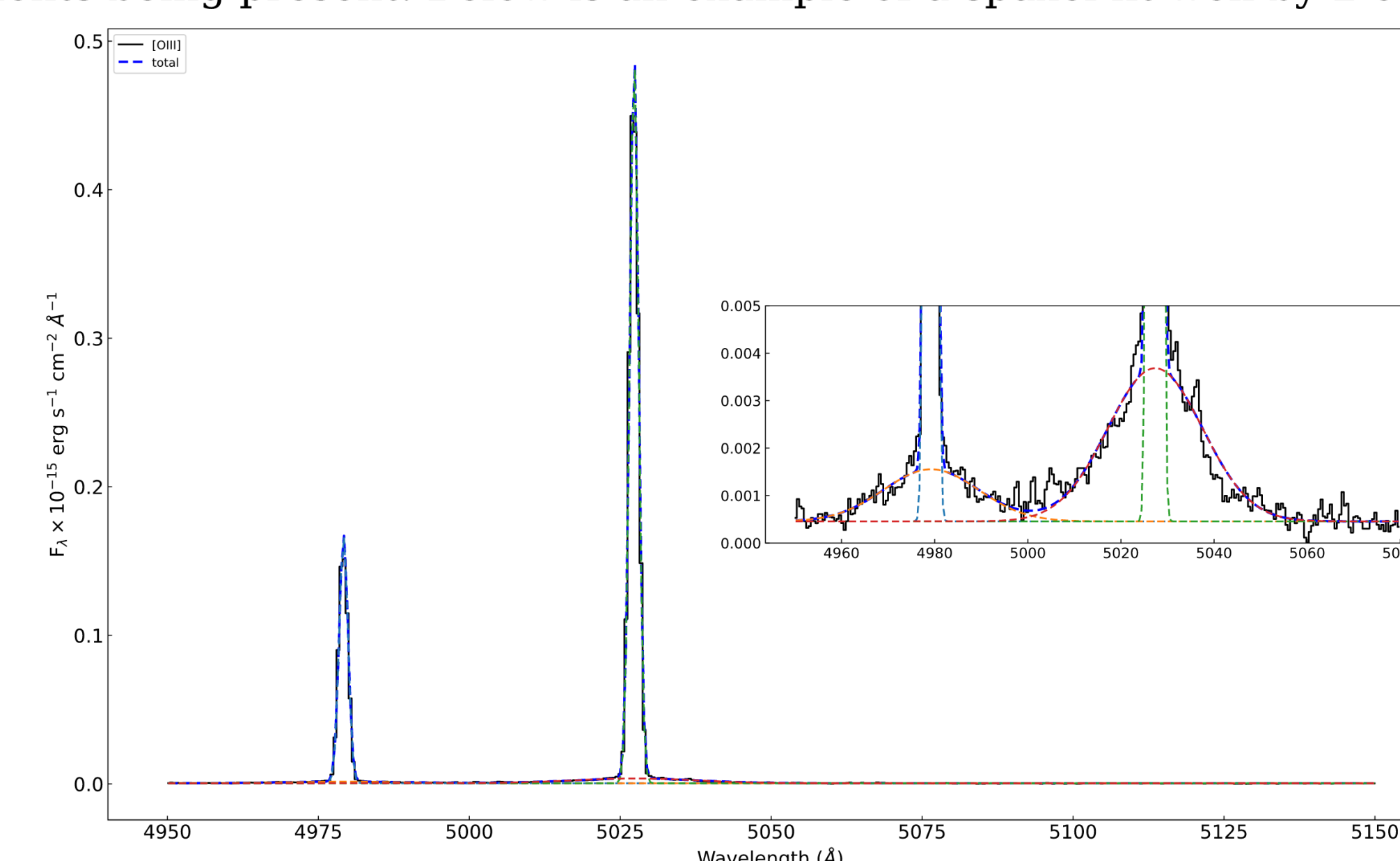
1. Pox 186 has an O_{32} ratio of ~ 20 [4], one of the most extreme values among the Green Pea sample. This implies a high ionization state in the majority of the ISM.

2. Its S/O ratio is high [4], likely stemming from a high ionization correction factor (ICF). Sulfur's ICF is dependent on O/O^+ , which is sensitive to the low ionization region at the edge of the H II as O^+ has a similar ionization potential to H^0 and O^0 . Being density bounded decreases the abundance of O^+ relative to O , therefore increasing O/O^+ and causing an overcorrection.

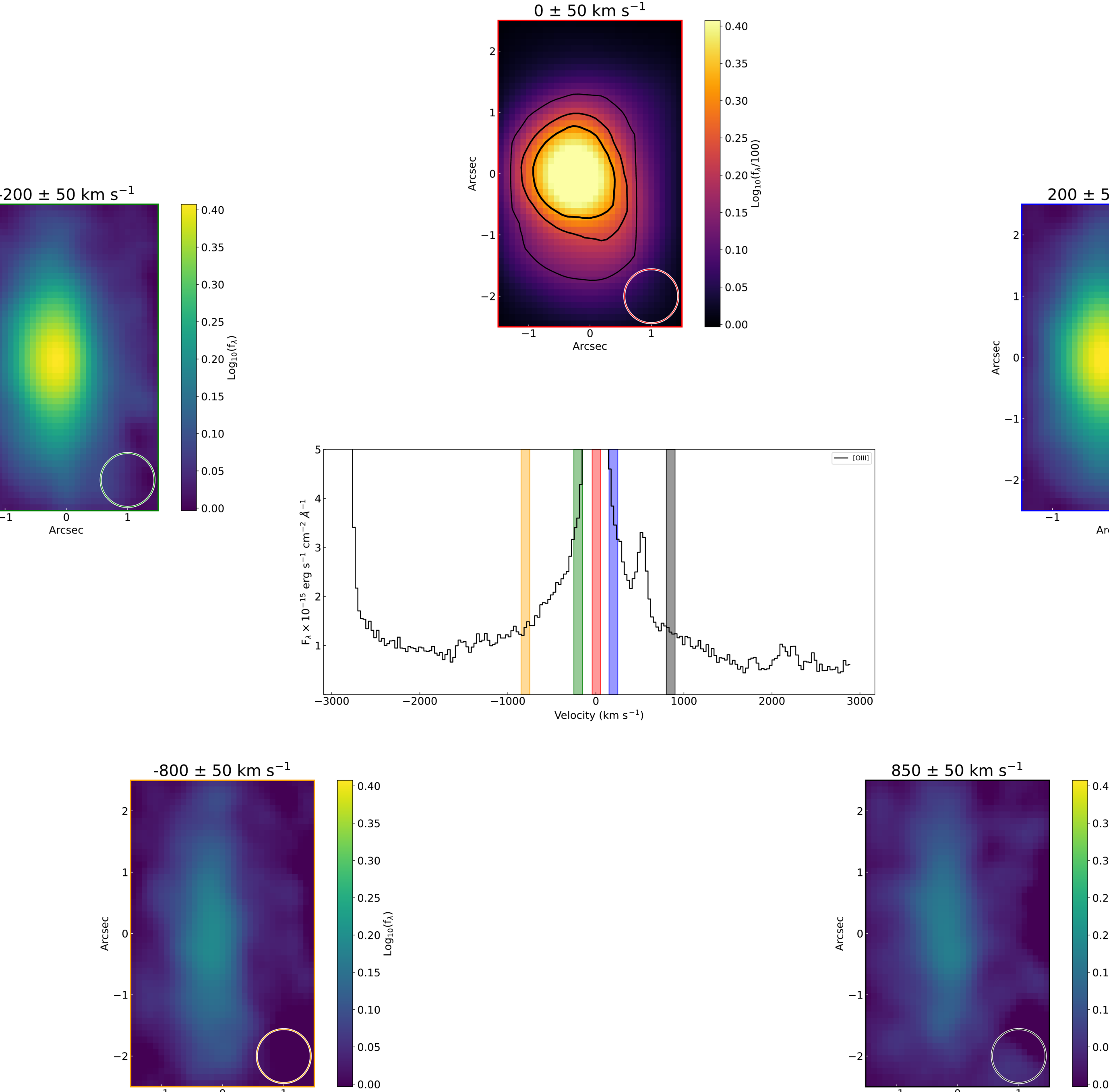
3. Pox 186 is undetected in $\text{H}\alpha$ 21cm with a 5σ upper limit of $M_{\text{HI}} < 1.6 \times 10^6 \text{ M}_\odot$ [5].

③ Data and Methods

We combine Integral Field Spectroscopy using the Gemini Multi Object Spectrograph at Gemini-South and Markov Chain Monte Carlo fitting to map kinematics of different gas components using the [OIII] 4959, 5007 doublet. The data show a changing kinematic landscape over the field of view. Some spatial pixels (spaxels) are fit well with one or two Gaussian components while others show signs of more than 2 components being present. Below is an example of a spaxel fit well by 2 components.

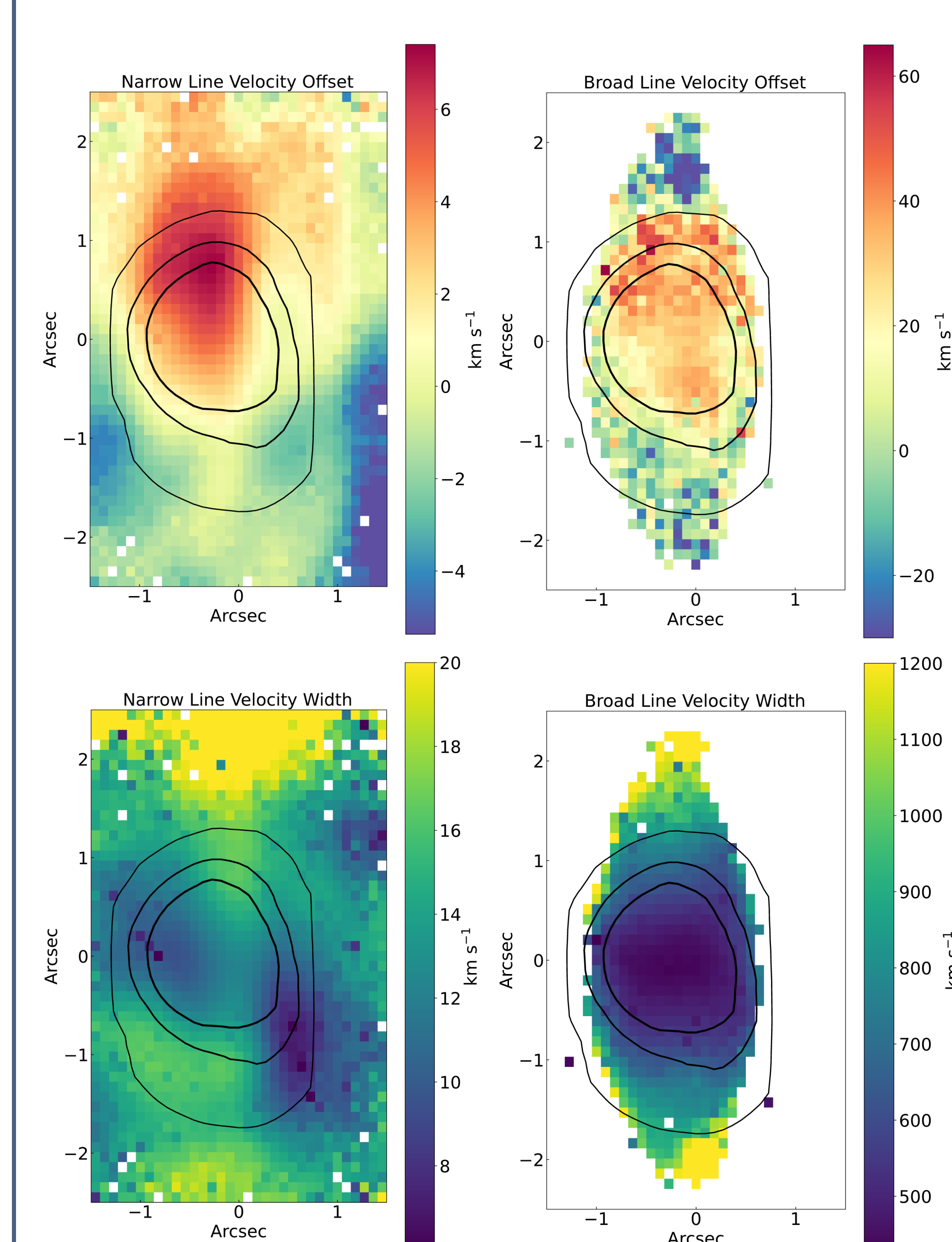


④ Morphology



Flux distributions from gas at different velocities. The central panel shows the 1-dimensional spectrum summed over all spaxels while the shaded bars signify the regions in velocity space used to create the surrounding images. The surrounding panels show the high velocity gas ($v > 50 \text{ km/s}$) has a distinctly different morphology as compared to the gas in the line center. Each outer image has been continuum subtracted. The colors of the bars match the outline of their corresponding image as well as the circle visible in the bottom right corner of each. The diameter of the circle denotes the full width max of the seeing, $.88''$. The upper central panel has been scaled by 100 to highlight that the [OIII] flux from high velocity gas is on the order of a few percent of the low velocity gas. The black contours are the same as in the HST image.

⑤ Kinematic Maps

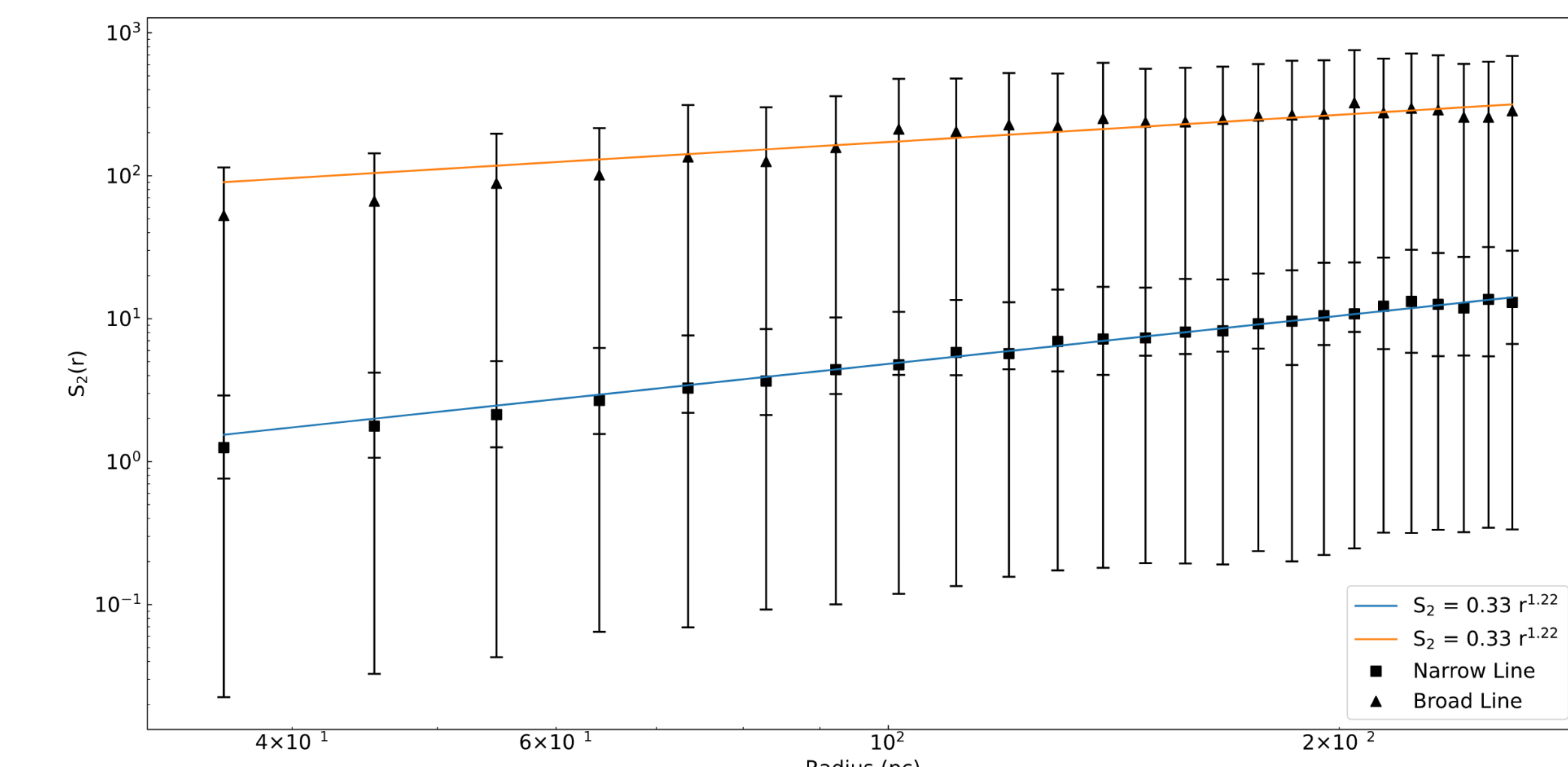


Maps of the MCMC fitting results. To allow for self-consistent comparisons between spaxels, all spaxels are fit with two Gaussian components while only those where the individual components have a $S/N > 3$ are shown. The velocity widths have been corrected for the instrument response and thermal broadening assuming a temperature of 17000 K and the black contours are the same as in the HST image.

⑥ Signs of "Leakiness"

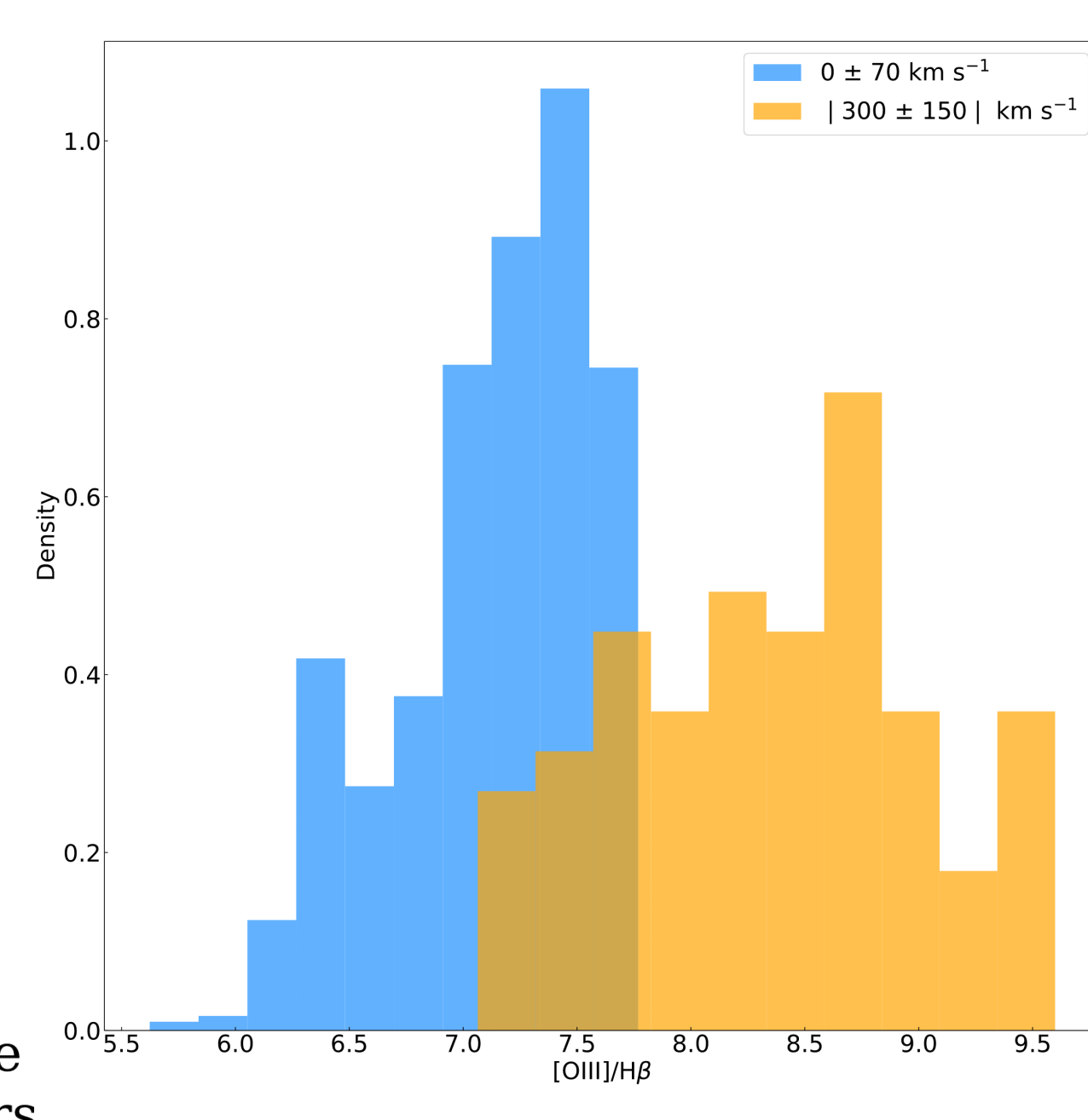
The driving force behind the broad component remains an open question. Its peculiar morphology suggests large scale outflows either in the form of jets or a biconical outflow due to stellar winds. We compare the [OIII]/H β ratio of gas at low velocities to high velocities (right) and find the high velocity gas consistently higher. Given the [OIII]/H β ratio is less than 10 implies a stellar ionization source based on the BPT diagram, which favors the stellar wind model of powering the broad component. The seeing, however, could be mixing an AGN-like source with surrounding star-formation, leading to lower [OIII]/H β ratios.

We also calculate an upper limit of the total mass of Pox 186 to be $\sim 2.5 \times 10^7 \text{ M}_\odot$ assuming a dark matter fraction of 90%. In this “best case” scenario, the escape velocity ranges from 25–50 km/s, implying nearly all of the broad component is being emitted by gas that will eventually escape the galaxy. This gas makes up a few percent of the total ionized gas mass.



Additionally, there is preliminary evidence of turbulence in both the broad and narrow components (left). We calculate the structure function, $S_2(r) = \langle [v(x) - v(x+r)]^2 \rangle$, where the error bars represent the dispersion at each radii, and find a positive slope of 1.22 for both components. This is indicative of turbulence, again favoring the stellar wind model. For reference, if the kinematic broadening was due to a virialized gas, the slope would be flat at small radii and taper off at large radii.

After a burst of star-formation, there exist many remnants of shells being blown out, colliding, and interacting with the wind in the form of turbulent mixing layers. Turbulence and colliding shells would increase the collisional rate which would explain the enhancement of [OIII]/H β as [OIII] is a collisional line.



References

1. Madau & Haardt 2015
2. Robertson et al. 2015
3. Izotov et al. 2018b
4. Guseva et al. 2004
5. Begum et al. 2005